



**HAL**  
open science

## Performance assessment of multi correlators interference detection and repair algorithms for Civil Aviation

Christophe Ouzeau, Christophe Macabiau, Benoit Roturier, Mikaël Mabillean

### ► To cite this version:

Christophe Ouzeau, Christophe Macabiau, Benoit Roturier, Mikaël Mabillean. Performance assessment of multi correlators interference detection and repair algorithms for Civil Aviation. ENC-GNSS 2008, Conférence Européenne de la Navigation, Apr 2008, Toulouse, France. hal-01022189

**HAL Id: hal-01022189**

**<https://enac.hal.science/hal-01022189>**

Submitted on 30 Sep 2014

**HAL** is a multi-disciplinary open access archive for the deposit and dissemination of scientific research documents, whether they are published or not. The documents may come from teaching and research institutions in France or abroad, or from public or private research centers.

L'archive ouverte pluridisciplinaire **HAL**, est destinée au dépôt et à la diffusion de documents scientifiques de niveau recherche, publiés ou non, émanant des établissements d'enseignement et de recherche français ou étrangers, des laboratoires publics ou privés.

# Performance Assessment of Multi correlators Interference Detection and Repair Algorithms for Civil Aviation

Christophe Ouzeau, *TéSA/ENAC/DTI*  
Christophe Macabiau, *ENAC*  
Benoît Roturier, *DSNA-DTI*  
Mikaël Mabileau, *Sofréavia*.

## BIOGRAPHY

Christophe OUZEAU graduated in 2005 with a master in astronomy at the Observatory of Paris. He started the same year his Ph.D. thesis on degraded modes resulting from the multi constellation use of GNSS, supported by DTI and supervised by ENAC.

Christophe MACABIAU graduated as an electronics engineer in 1992 from the ENAC in Toulouse, France. Since 1994, he has been working on the application of satellite navigation techniques to civil aviation. He received his PhD in 1997 and has been in charge of the signal processing lab of the ENAC since 2000.

Benoît ROTURIER graduated as a CNS systems engineer from Ecole Nationale de l'Aviation Civile (ENAC), Toulouse in 1985 and obtained a PhD in Electronics from Institut National Polytechnique de Toulouse in 1995. He was successively in charge of Instrument Landing Systems at DGAC/STNA (Direction Générale de l'Aviation Civile/Service Technique de la Navigation Aérienne), then of research activities on CNS systems at ENAC. He is since 2000 head of GNSS Navigation subdivision at DGAC/DTI (Direction de la Technique et de l'Innovation, formerly known as STNA) and is involved in the development of civil aviation applications based on GPS/ABAS, EGNOS and GALILEO. He is also currently involved in standardization activities on future multi constellation GNSS receivers within Eurocae WG62 and is the chairman of the technical group of ICAO Navigation Systems Panel.

Mikaël Mabileau graduated in 2006 as an electronics engineer from the Ecole Nationale de l'Aviation Civile (ENAC) in Toulouse, France. He is currently working for EGIS AVIA as a consultant engineer in the GNSS Navigation domain.

## 1. INTRODUCTION

Future GNSS combined receivers will have to be compliant with requirements that are defined by means of performances specified in terms of integrity, continuity, availability and accuracy for Civil Aviation community. The architecture of those receivers is currently defined from investigations about the advantages and risks linked to the multiple constellation use of GNSS signals. The different means identified by EUROpean Organization for Civil Aviation Equipment WG 62 to provide aircraft position and integrity during an aircraft all phases of flight are Galileo (E1, E5), GPS (L1, L5), GIC, SBAS(L1, L5) and RAIM algorithms.

The objective is to provide, as far as possible, position and integrity to a flying aircraft under all kinds of external conditions (dynamics, multipath, interferences...) for all phases of flight and even the most restrictive ones in terms of requirements.

GNSS components (constellations, frequencies) combinations will provide different levels of performance compared with the targeted phase of flight requirements.

From the level of performance that can be reached by the proposed GNSS components, operational combinations are classified into modes of operation. Each mode is identified by taking into account the fact the level of performance is compliant or not with the requirements for each phase of flight.

Thus, nominal, alternate and degraded modes characterize the identified associations. Combinations that allow reaching the specified requirements linked to a phase of flight are included in nominal and alternate modes. Nominal means are preferred to alternate ones for various reasons as explained in [EUROCAE, 2007].

If all those nominal and alternate combinations are unavailable, the use of remaining components is identified as a degraded mode.

Consequently, to take full benefits of all available GNSS components, WG 62 proposed a

switching architecture between nominal, alternate and degraded combinations.

To initiate a switch between currently used components and other ones, unavailability of the current ones must be declared. This unavailability follows a degradation occurring on one of the running components.

A flag of degradation must be raised, when appropriate, by monitoring parameters that could be affected by phenomena encountered in GNSS and Civil Aviation. To do that, detection means and more precisely, criteria on the identified parameters have to be established. Detection means can be based on observations made in the front end level, within tracking loops or on pseudorange and integrity information for instance.

Amongst the most feared physical phenomena that could lead to degradation, and thus, a loss of component, interferences have to be monitored. Indeed, this phenomenon can affect simultaneously several GNSS measurements.

Future combined GNSS receivers will have to be robust against interferences with a certain power.

It is all the more important to develop such receivers for Civil Aviation community since interferences can lead to an increased noise, a bias or a loss of pseudoranges, and thus a degraded navigation solution. In addition, interference types are various as we explain hereafter.

Interference environment includes pure carriers, narrow bands and pulsed interferences signals. For instance, a listing of identified interference sources was made by RTCA (SC 159, WG 6) in [RTCA, 2002], appendix B for GPS L1 C/A signal.

On going studies on the detection and removal of pulsed interferences are being conducted at RF front-end level for instance in [Raimondi, 2006].

For Civil Aviation applications, interferences with power level below the masks are expected to generate acceptable degradations on tracking errors.

We have shown that, even below the RFI mask, in certain conditions, the tracking errors induced by CW can be larger than expected by EUROCAE ([EUROCAE, 2007]).

This is all the more important for highly restrictive approach phases of flight in terms of accuracy. That is why this study focuses on detection of CW and on repair.

This paper starts with a quick description of the receiver general environment. Civil Aviation requirements are recalled. Then, assumptions about signals, interferences and the way to detect interferences are described; results are discussed and compared with ICAO requirements. Finally, a repair algorithm based upon a Prony-like method is tested.

## 2. ASSUMPTIONS AND SETTINGS

It is supposed in [EUROCAE, 2007] that interferences can affect signals received by future combined receivers inside an aircraft. Consequently, the requirements for each phase of flight must be respected whatever the aircraft environment.

According to [EUROCAE, 2007], the level of performance expected while losing L1 C/A or E1 and consequently GPS or Galileo services, is only compliant with non-restrictive En-route to NPA phases of flight, [EUROCAE, 2007].

As a consequence, it is of interest to test detection algorithms taking into account APV phases of flight which are the first restrictive approach phases of flight that require vertical guidance and follows NPA phase of flight. For sake of understanding, those requirements are recalled hereafter:

	NPA	APV I
Accuracy hor.	220 m	16 m
Accuracy ver.	x	8 m
Integrity	$10^{-7}/h$	$2.10^{-7}/app$
TTA	10 sec	10 sec
$P_{FA}$	$3.33.10^{-7}$	$1.6.10^{-5}$

Table 1 : Civil Aviation Requirements for NPA and APV I phases of flight.

Different ways to detect interferences are identified; it can be done at front end level and within tracking loops for instance in [Bastide, 2001], [Ouzeau et al., 2008] or [Raimondi, 2008].

This study focuses on the detection within tracking loops, and more precisely, on the monitoring of the correlator outputs.

In this study, the power of the generated CW is chosen below the interference masks provided in [EUROCAE, 2007]. The largest CW interference power used for detection tests is -155 dBW.

In this paper, only GPS L1 C/A and Galileo E1 code spectrum lines are supposed to be affected by CW interferences.

Useful signals (L1/E1) are assumed to be affected by a level of noise equal to -203 dBW/Hz and the received power for each case is provided in the following table:

	GPS L1 C/A	GALILEO E1
C/N0 (dB Hz)	40.5	34.8
Received power	-164 dBW	-168 dBW
Noise level	-203 dBW	-203 dBW

Table 2 : Minimum required carrier to noise ratios for GPS and Galileo signals from [EUROCAE, 2007], appendix H.

The priority is to be able to detect CW interfering with L1 C/A and E1 signals as it is the major jamming risk for those signals. Due to their frequency occupation on the same band than DME, L5 and E5 signals major threats are pulsed interferences. Consequently, the priority for those signals is pulsed interference detection and mitigation as it is currently studied in [Raimondi, 2008]. As a consequence, those signals are not studied here; the priority is given to L1 C/A and E1.

The detection is made during the tracking process which characteristics are provided in the following table:

	CHARACTERISTICS
DLL	1 <sup>st</sup> order, Bw: 1 Hz, dot product discriminator
PLL	3 <sup>rd</sup> order, Bw: 10 Hz, arctan discriminator
Integration time	L1 C/A, data ch: 20 ms, pilot: 4 ms, E1, data ch: 100 ms, pilot: 4 ms.

Table 3 : tracking characteristics.

The interference is supposed to impact GPS L1 C/A and Galileo E1 signals which do not have the same spectrum properties (line spacing, amplitudes). It is of interest to consider the high amplitude code spectrum lines for each PRN in order to quantify this impact on the resulting tracking loop error. Obviously, this error differs from one affected code spectrum line to another one. It is expected that the higher the amplitude of the spectrum line, the higher the resulting tracking error.

A model of the impact of CW suggests that the resulting tracking error of these interferences can be larger than assumed so far in previous studies. The impact of those interferences on correlators outputs are described in [Bastide, 2001], but this paper does not describe their impact on tracking

accuracy. The resulting tracking error can then lead to a large additive error on pseudoranges.

Hereafter are provided the highest GPS L1 C/A and Galileo E1 code spectrum lines, that is to say, having the highest power, likely to generate the highest tracking and positioning errors.

	GPS L1 C/A	GALILEO E1
Power	- 21.29 dB	- 28.81 dB
Frequency	227 kHz	673.5 kHz
PRN	6	38

Table 4 : Highest GPS L1 C/A and Galileo E1 code spectrum lines of PRN 6 and 38 (respectively)

It is of interest to consider the receiver environment as it determines the conditions of interference detection. To comply with APV conditions, dynamics and multipath have been generated as explained in [Ouzeau et al., 2008]. Dynamics were generated according to [EUROCAE, 2007] specifications.

Two types of dynamics are considered: normal and abnormal aircraft manoeuvres with corresponding aircraft maximum speed, acceleration and jerk. When it is not mentioned, aircraft dynamics are set to the normal case in this paper as defined in [Ouzeau et al., 2008]. Indeed, as mentioned in [RTCA, 2006]: "During abnormal manoeuvres, the receiver shall continue to provide a position output, it shall not output misleading information and the alerting mechanism shall function as normal. [...] During abnormal manoeuvres, the receiver is not required to meet the accuracy requirement." As a consequence, accuracy of our algorithms is not discussed here in case of abnormal dynamics.

Multipath were generated thanks to Aeronautical Channel model proposed by [Lehner, 2007] considering a 10 degree elevation of satellites. The aircraft is supposed approaching a targeted airport. A jammer is supposed to be located on the Earth, about 20 km away from the aircraft.

Generally, multipath have a significant impact on correlators as they use to distort the correlation peaks. However, as it is shown in [Ouzeau et al., 2008], and demonstrated through simulations using the proposed Aeronautical Channel model, during APV, multipath do not have a significant impact on interference detection as they do not disturb the correlation peaks enough.

Taking into account all those APV conditions, interference detection capability of the following proposed algorithms have to be discussed. Indeed, it has to be compliant with false alarm rate imposed by APV (see Table 1) and missed detection probability has to be determined to know if the proposed algorithms reduce significantly the

integrity risk due to interferences or not. If a CW with a high power is not detected, what is the resulting tracking error? Does it exceed the requirements?

### 3. DETECTION ALGORITHMS

Interference detection criteria described further are based upon the monitoring of the correlator outputs because the correlation between a sine wave and PRN code is still a sine wave and as a consequence, the occurrence of a CW results in the appearance of a sine wave in the correlator output as depicted in Figure 1. The amplitude of the wave is dependent upon the amplitude of the jammer, the amplitude of the hit code spectrum line and the frequency offset between the jammer and the nearest code spectrum line.

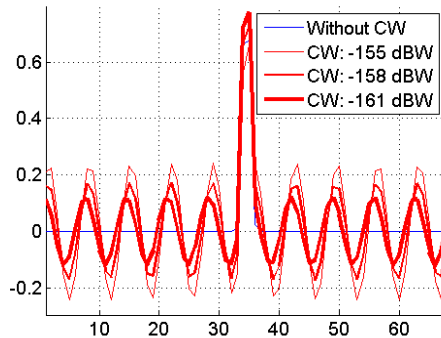


Figure 1 : GPS L1 correlator output, without and with different amplitude CW on the I channel

Indeed, detection depends upon the sinusoidal behaviour of the correlators outputs shape, resulting from the correlation between code and interference. The correlation between code and interference is expressed, for both I and Q channels, by the following expressions:

$$\begin{cases} R_I(\hat{\tau}, n) = \frac{A_J}{2} \sum_{k=(n-1)M}^{nM-1} \cos(2\pi\Delta f k T_s - \theta_j + \hat{\theta}) C(kT_s - \hat{\tau}) \\ R_Q(\hat{\tau}, n) = \frac{A_J}{2} \sum_{k=(n-1)M}^{nM-1} \sin(2\pi\Delta f k T_s - \theta_j + \hat{\theta}) C(kT_s - \hat{\tau}) \end{cases}$$

Where:

- $n$  is the temporal index of the I&D outputs
- $\hat{\theta}$  is the estimated phase tracking
- $\hat{\tau}$  is the estimated code tracking
- $M$  is the number of summed samples by I&D
- $\theta_j$  is the jammer shift
- $A_J$  is the jammer amplitude
- $T_s$  is the integration time and  $F_s=1/T_s$  is the sampling frequency
- $\Delta f$  is the frequency shift between the intermediate frequency and the jammer after the RF front-end

- $C$  is P/NRZ/L waveform associated to navigation message and code (C/A for instance)

GNSS receivers have several reception channels. Each of them specializes in tracking specific satellites. Each reception channel has at least two or three pairs of correlators (Early, Late, Prompt) for both code and carrier phase tracking.

A multi correlator receiver can compute much more correlator outputs in a same reception channel. If several correlators are available within a same channel, it is possible to observe the code autocorrelation value in several points spaced by a value denoted  $d$ .

In the following, multiple correlators outputs are monitored to detect the presence of jammers.

The correlators spacing  $d$  and the correlators window size around the main peak for both GPS and Galileo signals have to be set.

For GPS L1 C/A, with a classical BPSK (1) modulation, the maximum CW frequency is 1.023 MHz, which corresponds to the main lobe of the signal spectrum, where the highest amplitude spectrum lines are located. The problem of detection out of this lobe is thus not addressed here.

The larger the chip range used for correlators, the better the identification of a CW. Indeed, the variations of a sinusoid are visible on a larger window in this case. So low frequency CW can be detected and estimated easily. As the maximum CW frequency is set to 1.023 MHz (denoted  $F$  in the following), the minimum required window size is 20.46 chip. In simulations, it is set to 22 chip. The total number of correlators used is  $2*34=68$  (considering both sides of the correlation peak).

The impact of CW on the correlator outputs for GPS L1 C/A and Galileo E1 signals has the same shape, that is to say a sine wave appears in the autocorrelation. But, as Galileo E1 code spectrum properties are different of GPS L1 C/A (two main lobes between -2MHz and 2MHz appear in the code spectrum whose lines are 250 kHz-spaced), another setting for correlators window size and spacing is required. As the worst PRN code lines are located on the main lobes of the spectrum, in this case,  $F=2$  MHz. The correlators spacing is set to 0.25 chip. Finally, the window size is set to 9 chips for the Galileo case. The total number of correlators is  $2*36=72$ .

Hereafter are proposed two detection algorithms using different techniques based on the monitoring of multiple correlators outputs. The first objective of such a study is to find the most robust detection algorithm against all kinds of external perturbations like multipath, high dynamics... but also to find the most appropriate and promising technique making a trade off between complexity and reached performance. Indeed, detection

algorithms with low complexity have to be implemented in order to have the simplest receivers architecture as possible.

The two proposed algorithms take advantage of the behaviour of correlators outputs while interference occurs. Both algorithms are based on the detection of a sine wave on the correlation.

The first proposed algorithm is based upon the computation of the FFT of the correlator outputs, to detect the presence of a sine wave in the spectrum.

The second algorithm monitors after each integration period the residual error of a vector AR model of the set of the correlator outputs. In other words, a multichannel AR algorithm is used to model simultaneously all correlators outputs and thus, to take advantage of the existing correlation between all correlators time variations linked to the sine wave around the correlation peak. In absence of jammer, those outputs are only subject to noise and multipath.

**Algorithm 1: computation of the FFT of the correlators outputs**

Using this algorithm, the presence of interferences in the incoming signal is detected thanks to the computation of the Fourier Transform of the correlators outputs as described in [Bastide, 2001]. If undesired carrier sine waves are present, degradation is flagged.

The maximum Fourier transform of the correlators outputs is compared to a threshold. If a significant sine wave distorts the correlators outputs, the maximum of the Fourier transform of the correlators outputs increases, and, in the case the threshold is well chosen, this interference can be detected. The mean and the standard deviation of the maximum Fourier transform are estimated during a training stage, while no interference occurs, under normal aircraft dynamics and APV multipath conditions.

The threshold is determined thanks to the false alarm rate provided for an APV phase of flight (Table 1) and set as a statistical percentile of the test distribution in presence of noise and multipath.

Then missed detection probability is estimated generating interferences over a large number of tests (at least  $10^5$ ) using the instantaneous Fourier transform of the correlators outputs and the mean and sigma values estimated during the training stage.

Detection is declared when the following condition is reached [Bastide, 2001]:

$$|\max\_fourier_{inst} - \text{mean}(\max\_fourier)| \geq \text{threshold} \times \text{std}(\max\_fourier)$$

Where :

- $\max\_fourier_{inst}$  is the maximum of the Fourier transform at a considered instant
- $\text{mean}(\max\_fourier)$  is the mean of maxima of the Fourier transforms during the training stage
- $\text{std}(\max\_fourier)$  is the standard deviation of the maxima of the Fourier transforms during the training stage
- $\text{threshold}$  is the chosen threshold for detection

**Detection performance compared to civil aviation requirements**

The obtained missed detection probabilities do not depend significantly upon the impacted code line using this FFT detection method. For a same given -155 dBW interference, testing different hit PRN worst code lines, the obtained  $P_{MD}$  do not differ significantly. Indeed, within the main spectrum lobes, the amplitude difference between the most powerful rays by PRN is around 3 dB for L1 C/A and 2 dB for E1 as shown in [Ouzeau et al., 2008].

The obtained missed detection probability under multipath and normal dynamics, generating -155 dBW CW is around  $6.66 \cdot 10^{-5}$  for all impacted GPS and Galileo code spectrum lines chosen with the highest amplitudes amongst PRN code lines.

We discuss now the impact of non-detected CW on the tracking errors for varying interference amplitudes.

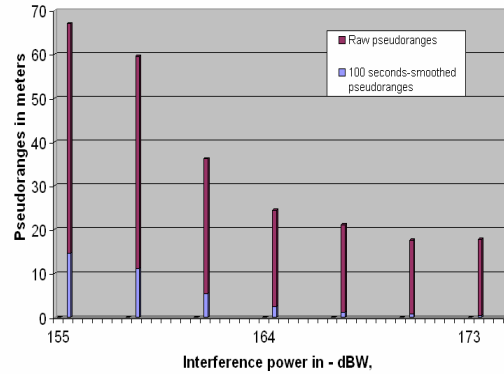


Figure 2 : Smoothed and raw maximum tracking errors for GPS L1 C/A PRN 6 for non-detected CW

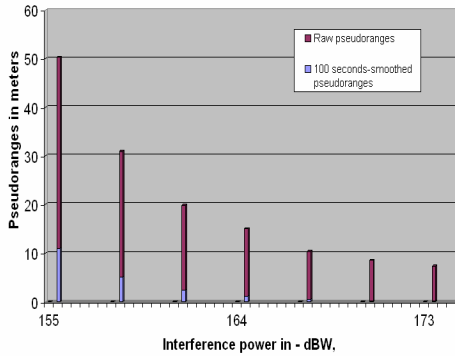


Figure 3 : Smoothed and raw maximum tracking errors for GPS L1 C/A PRN 2 for non-detected CW

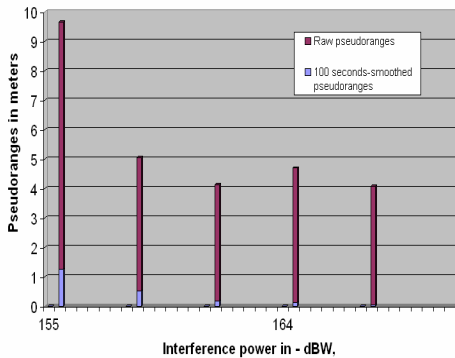


Figure 4 : Smoothed and raw maximum tracking errors for GALILEO E1 PRN 38 for non-detected CW

Several CW interference with different powers are generated. Figures 2, 3 and 4 show the raw and smoothed code obtained when interference is not detected. This was done for both GPS and Galileo signals. Code tracking errors were represented without (in pink) and with (in blue) smoothing by a Hatch filter with 100 seconds time smoothing constant.

It can be seen that for the worst case GPS PRN code spectrum line amplitude (on PRN 6), a -155 dBW interference power can generate a raw error of more than 60 meters reduced to less than 15 meters after 100 seconds carrier-phase smoothing. For other code spectrum lines (like for one PRN 2 code line impacted plotted above), the resulting tracking error while CW is not detected, is lower. For PRN 2, the raw error is 50 meters for the worst case -155 dBW CW reduced to 10 meters after smoothing. As expected, this error decreases with the CW amplitude.

The same test was conducted for future Galileo E1 signals (Figure 4). It can be seen that for the worst case PRN code line, the resulting non-detected maximum tracking error is around 10 meters and over 1 meter after smoothing as it can be seen Figure 3 and Figure 4.

As the algorithm missed detection probability is low compared to the number of

samples tested, the number of examples of tracking errors obtained during missed detection is low. As a consequence, those results have to be taken with care. The maximum tracking errors are obtained amongst a low number of available measurements.

With a large number of tests, it will be interesting for future works, to plot the distribution of the tracking errors resulting from the non-detected CW.

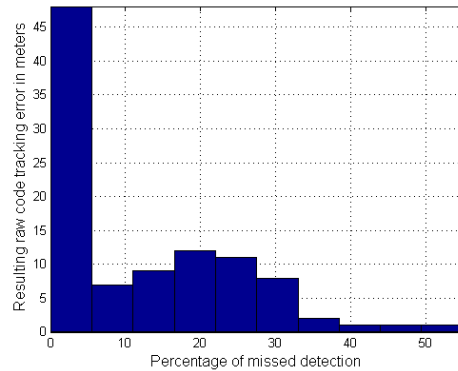


Figure 5 : Percentage of obtained missed detection classified by resulting raw tracking errors for GPS L1 C/A PRN 6 highest code spectrum line impacted by a -155 dBW CW interference, over  $3 \cdot 10^6$  tests.

However, we provide here some preliminary results represented Figure 5 over  $3 \cdot 10^6$  tests of the resulting raw tracking errors distribution. Those results have been obtained for GPS L1 C/A PRN 6 highest code spectrum line impacted by a -155 dBW CW interference.

As a conclusion, this detection algorithm is expected to alleviate RAIM-type algorithms, APV required integrity being  $2 \cdot 10^{-7}$  as recalled in Table 1. The obtained  $P_{MD}$  value is around  $6.66 \cdot 10^{-5}$  for the worst case CW amplitude for both GPS and Galileo cases.

### Algorithm 2: multichannel autoregressive model of correlators outputs

This proposed algorithm is based on the detection of non regular time variation of an AR model of the set of the correlation outputs. The residuals of the model are then monitored.

The correlators outputs are supposed to be affected by white Gaussian noise and multipath when no interference occurs.

Interferences do not imply a constant additive jump on the correlators outputs but they imply a time-varying additive jump.

If a CW interferes with the incoming signal, then the variance increases exactly when the interference occurs and varies abnormally during the period the signal is jammed.

Time variations of each correlator output are modelled thanks to an AR filter and the residuals of the model is monitored:

$$e[n] = x[n] - \hat{x}[n] = x[n] + \sum_{k=1}^p a[k]x[n-k]$$

Where:

- $n$  is the time index
- $e$  is the model error
- $x$  is the observed sequence of each correlator output
- $\hat{x}[n]$  is the linear prediction estimate of the sample  $x[n]$

For a first approach, it is not necessary to model the correlators outputs time-behaviour thanks to an ARMA model.

A classical AR model could have been used to monitor independently each correlation point, but it is preferable to use a multichannel AR model that helps having redundant information about all correlators behaviour, on the peak and beside it. Indeed, in presence of jammer, all correlators are affected by sine waves. Correlators time variations are linked by the CW characteristics.

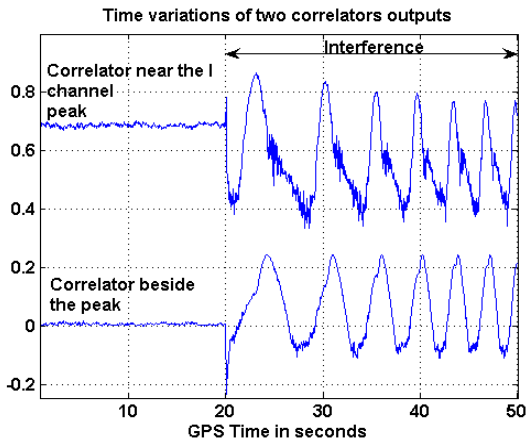


Figure 6 : Time variations of correlators for GPS L1 C/A signal

Using this technique, when interference occurs, the existing correlation between all correlators outputs as it can be seen on Figure 6, is exploited in presence of GNSS signals, noise, multipath and obviously, interferences.

The model residuals are monitored thanks to the following criterion calculated:

$$\log \frac{AR\_model\_error}{previously\_estimated\_AR\_model\_error}$$

- The numerator is the instantaneous AR model error, updated for each test and for each correlator.

- The denominator is determined through a training simulation without interferences and under the phase of flight conditions as for the FFT algorithm, before the detection tests.

### Test distribution

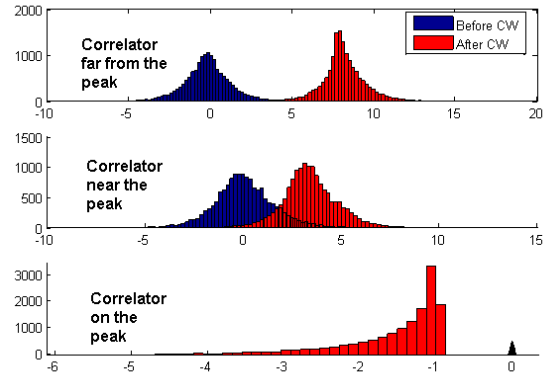


Figure 7 : AR test distribution for three channels (three correlators), in blue without CW and in red with CW

On Figure 7 are represented the distribution of the test criterion on some correlator outputs and over  $1.5 \cdot 10^5$  tests without interference in blue and with interference in red.

It can be seen on Figure 7 that even if correlators have the same behaviour when interference occurs, the gap between model errors differs from one channel to another one.

### Detection performance compared to civil aviation requirements

The obtained  $P_{MD}$  using this technique is near  $10^{-5}$  considering the worst case GPS PRN 6 code spectrum line and -155 dBW CW interference. The detection capability of this algorithm is slightly higher than the first proposed algorithm but it requires a multichannel correlator Auto Regressive model. As mentioned for the first proposed algorithm, this technique, elaborated here for interference detection, is expected to alleviate RAIM-type algorithms.

Future works will consist in taking into account both detection capability within tracking loops using the proposed techniques and the RAIM capability to detect failures due to interferences to discuss more precisely the interests of implementing such detection algorithms within future GNSS combined receivers. More precisely, it is of interest to know the resulting performances of combined interference detection algorithms and RAIM during APV, while generating CW impacting worst case code lines.

In addition, future studies will consist in analyzing the proposed algorithms implementation cost.



#### 4. CORRELATOR OUTPUTS REPAIRS AND RESULTING TRACKING PERFORMANCE

It is of interest to know the performance of a repair algorithm when interference is flagged, because when interference detection is successful, interferences impact on tracking should be reduced or removed with a low complexity algorithm as described hereafter.

In order to repair the correlators outputs, interferences characteristics have to be determined. To do that, several methods could be found in literature and we mention the most popular ones.

The FFT is a basic tool for spectral analysis of interferences. It is well-known as a powerful method that has a low calculation cost, interesting for processing of a broad range of signals. In addition, it is robust and resistant against noise. However, this well-known technique has a too low 1/N-resolution, where N is the number of samples used. Indeed, for a low number of samples, this technique is not applicable to our problem.

Parametric models allow representing physical phenomena like CW interfering signals. Such models provide, with a small number of parameters, the principal characteristics of a CW, like its amplitude and phase. It is consequently a good mean to reduce the calculation cost associated with the signal process. Moreover, those techniques need fewer points for a same resolution as the FFT. That is why, in the following, a Prony model is used to characterize the CW interferences.

The first step consists in estimating the poles  $Z_k$  of the parametric model. Using the AR model, it can be shown that the  $Z_k$  are the roots of the following polynomial:

$$A(Z) = \sum_{k=0}^p a_k Z^{-k}$$

From the  $Z_k$  values, it is easy to deduce the associated damping factor and the frequency:

$$\alpha_k = \frac{\ln|Z_k|}{T}$$

And:

$$f_k = \arctg\left(\frac{\text{Im}(Z_k)}{\text{Re}(Z_k)}\right) / 2\pi T$$

The last step is now the estimation of the  $b_k$  values. To do so, the Prony model can be re-written as a vector product

$$V \underline{b} = \underline{X}$$

Where:

$$V = \begin{pmatrix} 1 & 1 & \dots & 1 \\ Z_1 & Z_2 & \dots & Z_p \\ \cdot & \cdot & \dots & \cdot \\ \cdot & \cdot & \dots & \cdot \\ Z_1^{N-1} & Z_2^{N-1} & \dots & Z_p^{N-1} \end{pmatrix}$$

$$\underline{b} = (b_1, b_2, \dots, b_p)^T$$

$$\underline{X} = (x(0), x(1), \dots, x(n-1))^T$$

The least square solution is given by:

$$\underline{b} = (V^H V)^{-1} V^H \underline{X}$$

The searched CW modules and phases can be then deduced by calculating:

$$A_k = |b_k|$$

$$\theta_k = \arctg\left(\frac{\text{Im}(b_k)}{\text{Re}(b_k)}\right)$$

A few results are presented in the following and concern the estimation and reparation when a CW hits the identified worst case GPS L1 C/A PRN 6 code spectrum line, located at 227 kHz.

In Figure 8 is represented the estimation of the CW frequency (227 kHz) over 100 tests thanks the proposed Prony model described previously. The obtained estimations are between 226.84 kHz and 227 kHz. The obtained resolution of the algorithm is consequently less than 200 Hz.

This simulation has been conducted assuming there is no Doppler effect between the jammer and the GPS code, so as to determine precisely the algorithm capability to estimate CW frequency.

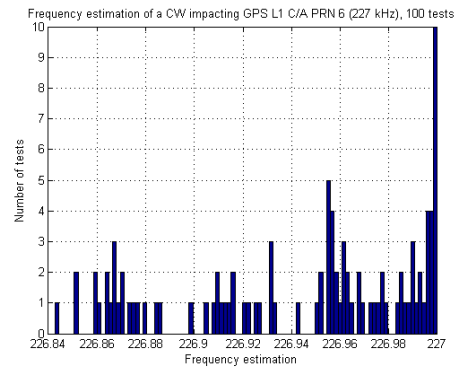


Figure 8 : Estimation of a -155 dBW CW frequency impacting GPS L1 C/A PRN 6 (227 kHz)

The frequency estimation is acceptable as it can be seen Figure 8, but the most important result is the resulting tracking error after reparation of the correlators outputs. Indeed, it can be noticed Figure 9 that this algorithm can provide significant improvement in tracking robustness and avoid a loss

of lock. Simulations show that the standard deviation of the code tracking error (always for GPS PRN 6), is reduced from 80 meters (in red) to 6 meters (in blue) in this case as it can be seen Figure 9.

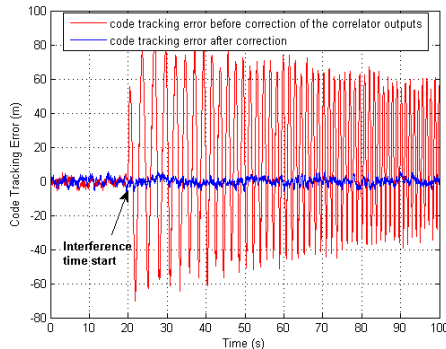


Figure 9 : Code tracking error before and after interference removal

## 5. CONCLUSIONS

During simulations, worst cases were considered in terms of interference power, code spectrum lines impacted, which makes the  $P_{MD}$  estimation robust against the mentioned interferences.

Two detection algorithms are proposed here and are expected to alleviate and complete the detection made by RAIM-type algorithms. The obtained  $P_{MD}$  are around  $10^{-5}$  for the worst case -155 dBW CW. Those results concern each worst case GPS L1 C/A PRN 6 and GALILEO E1 PRN 38 worst case code spectrum lines using each of the two proposed detection algorithms.

The resulting maximum error on smoothed pseudoranges when no detection algorithm is used is around 15 meters for GPS L1 C/A and around 1 meter for Galileo E1.

The presented techniques are consequently useful when interference occurs during approach phases of flight like APV because, it allows detecting degradation due to a CW with a low  $P_{MD}$  (integrity) and in case of failure in the detection, the resulting error does not exceed 1 meter while using Galileo E1 for positioning. This error will not have a harmful impact on the aircraft position estimation in this case.

Those results have to be compared with RAIM detection capabilities.

When detection is made and when there is an impact on performances (accuracy), it is possible to repair data thanks to the characterization of interferences with a Prony-like model for instance. Interference effects can be removed in this case for accuracy purposes as proposed in this paper.

The repair algorithm provides good results as the maximum tracking error is reduced from 80 meters to 6 meters as shown Figure 9.

## REFERENCES

[Bastide, 2001] *F. Bastide*, GPS interference detection and identification using multicorrelator receivers, ION 2001

[Burnham, 2004] *Multimodel Inference: Understanding AIC and BIC in Model selection*, *Kenneth P. Burnham, David R. Anderson*, Colorado State University, 2004.

[EUROCAE, 2007] *Minimum Operational Performance Standards for Galileo*, EUROCAE, WG 62, 2007.

[Esbri, 2006] *Antenna-based Multipath and Interference Mitigation for Aeronautical Applications: Present and Future*, *O. Esbri-Rodriguez*, DLR German Aerospace Center, Germany, *M. Philippakis*, ERA Technology (Cobham PLC), U.K., *A. Konovaltsev*, DLR German Aerospace Center, Germany, *F. Antreich*, DLR German Aerospace Center, Germany, *C. Martel*, ONERA, France (formerly with ERA Technology (Cobham PLC), U.K.), *D. Moore*, ERA Technology (Cobham PLC), U.K., 2006.

[Holmes, 1990] *Coherent Spread Spectrum Systems*, Holmes, Krieger, 1990.

[Julien, 2005] PhD Thesis: Design of Galileo L1F Receiver Tracking Loops, *Olivier Julien*, July 2005.

[Lehner, 2007] *Multipath Channel Modelling for Satellite Navigation Systems*, *Andreas Lehner*, Shaker Verlag, 2007.

[Mabilleau, 2007] *Combined GALILEO-GPS receiver based on a switching logic*, *Mikaël Mabilleau (DTI)*, *Paul Nisner (NATS)*, *Laurent Azoulai (Airbus)*, *Jean Pierre Arenthens (Thales)*, *Gerard Alcouffe (Thales)*, *Christophe Ouzeau (ENAC)*, Navigation System Panel, New Delhi, India, March 2007.

[Macabiau, 2006] *GNSS Airborne Multipath Errors Distribution Using the High Resolution Aeronautical Channel Model and Comparison to SARPS Error Curve*, *Christophe Macabiau*, *Laetitia Moriella*, *Mathieu Raimondi*, ENAC/INSA, *Cyril Dupouy*, STNA, *Alexander Steingass*, *Andreas Lehner*, DLR, ION NTM 2006.

[Marple, 1987] *Digital Spectral Analysis With Applications*, *S. Lawrence Marple, Jr.*, Prentice Hall, Signal Processing Series, 1987.

[Ouzeau et al., 2008] *Performance of Multicorrelators GNSS interference Detection Algorithms for Civil Aviation*, *Christophe Ouzeau (TéSA)*, *ENAC*, *DTI*, *Christophe Macabiau (ENAC)*, *Benôit Roturier (DSNA-DTI)*, *Mikaël Mabilleau (Sofréavia)*, ION NTM 2008.

[Raimondi, 2006] Mitigating Pulsed Interference Using Frequency Domain Adaptive Filtering, *Mathieu Raimondi, ENAC/INSA, Christophe Macabiau, ENAC, Frederic Bastide, Sofreavia/DTI, Olivier Julien, ENAC, ION GNSS 2006.*

[RTCA, 2006] Minimum Operational Performance Standards For Global Positioning System/ Wide Area Augmentation System Airborne Equipment, RTCA Paper No. 093-06/SC-159-939, 2006.

[RTCA, 2002] Assessment of Radio Frequency Interference Relevant to the GNSS, DO-235A, RTCA SC-159 Inc, 2002.

[Steingass, 2004] The High Resolution Aeronautical Multipath Navigation Channel, *Alexander Steingass, German Aerospace Center DLR, Andreas Lehner, German Aerospace Center DLR, Fernando Pérez-Fontán, University of Vigo, Spain, Erwin Kubista, Joanneum Research, Austria, Maria Jesús Martín, University of Vigo, Spain and Bertram Arbesser-Rastburg, European Space Agency, The Netherlands, ION 2004.*

[Stephens, 1995] *S. A. Stephens, J. B. Thomas*, "Controlled-Root Formulation For Digital Phase-Locked Loops".